Spring 4-2017

Determination of the Zinc Concentration in Human Fingernails by Laser-Induced Breakdown Spectroscopy

Steven J. Rehse
University of Windsor

Vlora A. Riberdy
University of Windosr

Christopher J. Frederickson
NeuroBioTex Inc.

Determination of the Zinc Concentration in Human Fingernails by Laser-Induced Breakdown Spectroscopy.

Vlora A. Riberdy[a], Christopher J. Frederickson[b,c], Steven J. Rehse[a,*]

[a]Department of Physics, University of Windsor, Windsor, Ontario N9B 3P4, Canada

[b]NeuroBioTex, Inc., 101 Christopher Columbus Blvd, Galveston, Texas 77550, USA.

[c]The University of Texas Medical School, Galveston, Texas 77550, USA.

riberdyv@uwindsor.ca (V.A. Riberdy)

zincdoc@gmail.com (C.J. Frederickson)

[*]Corresponding author. Tel.: +1 5192533000 (x2656); fax: +1 5199737075.

E-mail address: rehse@uwindsor.ca (S.J. Rehse).

Abstract

The absolute concentration of zinc in human fingernail clippings tested ex vivo was determined by 1064 nm laser-induced breakdown spectroscopy and confirmed by speciated isotope dilution mass spectrometry. A nail testing protocol that sampled across the nail (perpendicular to the direction of growth) was developed and validated by scanning electron microscopy energy dispersive x-ray spectroscopy. Using this protocol, a partial least squares regression model predicted the zinc concentration in five subjects' fingernails to within 7 ppm on average. The variation of the zinc concentration with depth into the nail as determined by laser-induced

breakdown spectroscopy was studied and found to show no systematic variation for up to 15 subsequent laser pulses in one location. The effects of nail hydration (dehydrated and overhydrated) and nail surface roughness on the assay were investigated to explain an anomalously large scatter observed in the measurements. This scatter was attributed to the layered nature and the fibrous structure of the fingernails which resulted in non-uniform ablation as determined by scanning electron microscopy. This work demonstrates that a protocol consisting of low pulse energy (<10 mJ) 1064 nm laser pulses incident on human fingernail clippings in an argon environment can produce quantifiable zinc emission in the laser-induced plasma and the measured zinc intensity can be used to accurately predict the nail zinc concentration.

Index Headings: Laser-induced breakdown spectroscopy; LIBS; Fingernails; Zinc; Partial least squares regression

1. Introduction

Zinc is one of the most important nutritionally-obtained elements in the human body, playing an important structural role in proteins and figuring prominently in many important signaling pathways.[1] Zinc is a component of over 3000 different mammalian proteins and is found in every organelle of every mammalian cell type, as well as fluids such as semen, pancreatic juice, saliva, and tears.[2,3] Zinc deficiency is a leading cause of death among toddlers worldwide,[4,5] and remediation of such deficiency by detection and supplementation has been identified by at least one organization as the most cost-effective improvement to world heath one could make.[6]

Significantly, zinc is a critical component in the neurophysiology and pathology of signalling in the brain and the central nervous system (CNS).[2,7,8,9] Evidence indicates that brain zinc is involved in the development of dementia/Alzheimer's disease[10,11] as well as autism,[12] stroke, epilepsy, seizures, and a host of other pathologies.[1]

Traditionally, the diagnosis of zinc deficiency has been made by drawing 10 mL of venous blood (preferably in the morning after overnight fasting), separating out the serum, and measuring the serum zinc concentration by laboratory instrumental methods such as mass spectrometry or atomic absorption spectroscopy.[13,14] For at-risk populations, primarily in underserved countries and communities, these methods are clearly unsuitable. Even though dietary zinc supplements are relatively inexpensive and essentially completely safe (up to 10-20 times the minimum daily requirement is routinely used),[15] there is a general reluctance to prescribe or administer zinc supplements without some prior screening to detect deficiencies. Indeed, the screening of at-risk populations is essential, as indicated in the "best practices" paper produced in 2008 by the Copenhagen Consensus.[6] Furthermore, convenient and timely testing to determine the efficacy of supplementation is always desirable.

Serum zinc is known to fluctuate dramatically in circadian rhythms and in response to zinc-rich meals, therefore it is possible that fingernail zinc (like bone zinc)[16,17] could potentially be a superior measure of longer-term nutritional zinc status. The fingernail concentrations of elements or chemicals such as selenium, nicotine, mercury, and ethanol metabolites have been used successfully in prior work to determine past oral intake of those substances.[18,19,20,21] The concentration of zinc in hair (another keratinous tissue) has also been shown to reflect dietary

intake.[22,23] We have recently conducted a preliminary study linking fingernail zinc to blood serum in which the zinc measured in the fingernails of 30 elderly residents of a nursing home in Detroit was correlated with an assignment of "good zinc nutriture" or "poor zinc nutriture" based on their dietary phytate/zinc ratios obtained from serum.[24] This study also included 17 Pakistani children from a group classified as "undernourished" by their local clinicians and in this case fingernail zinc was found to also be a good predictor of the subject's zinc nutriture.

The concentration of zinc and other trace elements may be quantified in fingernails using traditional analytical technique such as inductively-coupled plasma mass-spectrometry[25] or x-ray fluorescence.[26] Each of these methods exhibits insufficiencies for this particular application including complexity, lack of portability, the necessity of chemical digestion, the use of ionizing radiation, and the requirement of clipping. It is our contention that the concentration of zinc as measured in the fingernail via laser-induced breakdown spectroscopy (LIBS) can serve as a surrogate assay for serum zinc concentration. A LIBS zinc assay on nails in situ could be done safely and virtually non-invasively, and could provide results immediately so that appropriate zinc intervention could be commenced. By performing point samples on the nail along the direction of nail growth this method could also be used to monitor changes in zinc nutriture over time due to supplementation. This was demonstrated in a year-long study we performed recently.[24]

LIBS has been utilized previously to elementally assay human fingernails[27] as a potential method for the quick determination of health problems such as hyperthyroidism and hypothyroidism,[28] the fungal infection onychomycosis,[29] and the identification of opium addicted subjects.[30] In these

studies, the elements Al, C, Ca, Fe, H, K, Mg, N, Na, O, Si, Sr, and Ti were routinely observed, but not zinc.

Rusack et al. utilized LIBS performed with a 1064 nm laser to study Mg, Ca, and Zn in human fingernails obtained from 11 subjects.[31] Utilizing the Zn I line at 481 nm, a calibration curve with an R^2 of 0.9896 was created after determination of absolute zinc concentration via atomic absorption spectroscopy. The authors noted a quite large relative standard deviation in these measurements (approximately 15-20% which is also observed in this study) due to the imprecise ablation of mass out of the highly-layered fingernail. They also concluded that pressed keratin pellets doped with zinc make poor test standard samples for the creation of a calibration curve to test a LIBS fingernail apparatus.

In this work, the quantitative measurement of Zn in the fingernails from five subjects was investigated via laser-induced breakdown spectroscopy. The variation in measured zinc amongst the fingers and between the left and right hand of each subject was investigated as was the effect of the state of hydration of the clipped nail. SEM analysis including energy dispersive x-ray spectroscopy was performed to better interpret the LIBS results. The zinc concentrations of nail clippings from the left hands of the subjects as determined by speciated isotope dilution mass spectrometry were used to prepare zinc calibration curves utilizing a multivariate partial least squares (PLS) regression. Nail clippings from the right hands of the subjects were used to test the PLS model which predicted the actual zinc concentration to within 7 ppm with an average standard deviation of 14 ppm. The fingernail content of subjects with low zinc nutriture can be as much as

50 ppm lower than that of subjects with exemplary zinc intake (unpublished results), therefore a 14 ppm uncertainty would still allow diagnosis of the severely deficient.

2. Materials and Methods

2.1 Equipment

The apparatus used to perform these LIBS experiments has been described in detail elsewhere.[32,33] A 1064 nm Nd:YAG laser (Spectra Physics LAB-150-10) with 10 ns pulses operating at 10 Hz was used in all experiments. Pulse energy was approximately 5 mJ/pulse. The pulses were focused by a high-damage threshold AR-coated 5× infinite conjugate microscope objective with a long working-distance (LMH-5X-1064, OFR). A CCD camera placed in line with this objective allowed observation of the nails as data was collected. An alignment helium-neon laser was used to visualize the laser beam focus on the sample (Fig. 1). Nails were held in the microscope objective focus on a steel sample holder inside a Plexiglas argon purge chamber mounted on a manual XYZ translation stage. During data acquisition, the chamber was flushed with argon at a flow rate of 20 SCFH.

Due to the curved anterior surface of the nail samples, horizontal translation of the nail sample caused the lens-to-sample-distance (LTSD) to vary, which, if unaccounted for, can add scatter to the LIBS measurements. To compensate for the curvature of the fingernail, a heavily attenuated secondary helium-neon laser (Uniphase Model 155A) illuminated the nail sample through the purge chamber wall at an angle of approximately 45 degrees. Changes of the LTSD due to nail curvature caused lateral motion of this secondary visible laser spot. This spot was used to

accurately and reproducibly adjust the LTSD to its nominal value, keeping the focal spot size of the LIBS laser constant.

Laser-induced plasma emission was collected and relayed to the spectrometer via two matched off-axis replicated aluminum parabolic mirrors (3.81 cm diameter, 5.08 cm effective focal length) which focused the light into a 1-m steel encased multimode optical fibre (core diameter = 600 μm, numerical aperture (NA) = 0.22). The fibre was coupled to an Echelle spectrometer equipped with a 1024×1024 pixel (24 μm^2) intensified charge coupled device (ICCD) camera (LLA Instruments, Inc., ESA3000). The spectrometer provided spectral coverage in the range from 200 to 840 nm and was controlled by a personal computer running manufacturer-provided software (ESAWIN v3.20) which controlled both the ICCD shuttering as well as the firing of the laser pulses.

2.2 Fingernail Specimen Collection

Nail samples were obtained from volunteers presenting no noticeable trauma or pathology to their nails. All samples were acquired in accordance with University of Windsor research ethics approval #32272. Nail clippings of the index, middle and ring fingers (both right and left hands) of five subjects were taken, providing a total of six nail clippings per subject. Clippings were cleaned with acetone in an ultrasound bath for ten minutes and allowed to dry for 20-30 minutes. Clippings were then cut into approximately two mm by two mm fragments to provide a flat target, as shown in Fig. 1. In the buffing study reported in section 3.5, nails were made smoother with an extremely fine grit titanium dioxide buffing board manufactured for use on fingernails. Prior to clipping, nails were buffed vigorously for 20 seconds then clipped and ultrasonically cleaned with acetone to remove any potential residue from the buffing board.

2.3 Optimization of LIBS Emission

Data were acquired by collecting the emission from ten sequential laser pulses in one location prior to a lateral translation of the nail (across the nail perpendicular to the direction of growth). Five such lateral locations were averaged in software to make one measurement spectrum (50 laser shots per spectrum). In our standard testing protocol and unless otherwise stated ten such spectra were averaged and the standard deviation of those ten measurements (500 laser shots total) was calculated to determine the average emission intensity and uncertainty of the measurements due to shot-to-shot variation. Because the image-intensified camera gain setting was variable, the observed emission intensity was relative and is reported here in arbitrary units (a.u.). All intensities reported here are background-subtracted integrated areas under the curve as measured by the ESAWIN software. To allow direct comparison of the data, once an appropriate gain setting was determined to utilize the maximum dynamic range of the camera without overflowing the CCD array, the gain was not changed for the duration of the study.

In one study, single shot spectra were acquired from 15 sequential laser pulses without translating the nail to determine if vertical depth effects due to the striated layered structure of the nails were measureable. Studies were performed to optimize the zinc emission intensity and signal-to-noise ratio. These studies indicated an ICCD camera delay time of 1 μs and an ICCD camera opening (integration) time of 5 μs provided optimal experimental conditions for testing in argon. Spectra were also acquired in air and helium, but possessed decreased intensity and signal-to-noise.

2.4 Hydration of Nails

The effect of the presence of liquid water in the nail specimen on the LIBS spectrum was investigated. In an attempt to over-hydrate a nail specimen, clipped nail samples from each of three volunteers were soaked in distilled water for approximately 1 week and were then dried under a cool air gun for 1 hour before being cut into segments and tested. As a control, nail samples from the same group of volunteers were cleaned in acetone before being air dried for 1 hour and then being cut into segments. These segments were then tested in the argon environment using the standard LIBS protocol described in section 2.3. Alternately, attempts were made to intentionally dehydrate the nails. Clipped, cleaned, and segmented nail samples from three volunteers were heated in a 122°C oven for approximately 48 hours to drive off water in the nails. Once removed, the nails were kept in a desiccator to prevent any moisture from returning prior to LIBS testing.

2.5 Scanning electron microscopy

Scanning electron microscopy (SEM) studies were performed using a low-vacuum environmental SEM (Quanta 200 FEG, FEI) without carbon or gold coating. Nail samples and a piece of stainless steel plate used for daily spectral calibration of the spectrometer system were imaged to compare ablation performance and crater size. The SEM was equipped with an energy dispersive x-ray spectroscopy (EDS) apparatus which was used to make zinc concentration point measurements and line measurements on nail sections by monitoring the zinc K-alpha line.

3. Results and discussion

3.1. LIBS Spectra

Fig. 2a shows a typical nail spectrum acquired in argon using the experimental parameters described in Section 2.3. The strongest observed emission features have been identified along with the center wavelength of the emission line. Along with the zinc analyte lines, the dominant emission was attributable to the carbon 247 nm line from the nail keratin and the spectroscopically intense emission lines from the ions of the metals calcium and magnesium, present in the nail at concentrations of approximately 2310 ppm and 570 ppm, respectively.[34] The strong hydrogen alpha line at 656 nm is unobserved in the spectrum due to the presence of a spectral gap in the Echelle spectrometer's wavelength coverage (no light is recorded in these spectral gaps.) Therefore this line commonly associated with the presence of water molecules could not be used to directly monitor fingernail hydration status. Figs. 2b, 2c, and 2d show the spectrum in the regions of the strongest zinc emission lines from the singly-ionized Zn^+ ion (Zn II 202.547 nm and Zn II 206.200 nm) and the neutral zinc atom (Zn I 213.855 nm). Due to the intensity and the reduced shot-to-shot variation of the Zn II emission the sum of the integrated areas under the background-subtracted curve of the two Zn II lines was used in all experiments as the measurement of the LIBS zinc intensity. The use of other emission lines, including the intense C I 247.856 line, for normalization was investigated but did not result in any improvement in precision or accuracy.

3.2 Effect of Lateral Translation and Depth Measurements

To determine if the data collection procedure described in section 2.3 was appropriate, studies were undertaken to search for any indication of a dependence of the measured LIBS zinc emission intensity on the lateral position across the nail or depth in the nail. Fig. 3a shows the lateral scan direction and the result of ten sequential measurements across the nail (perpendicular to the direction of growth) with ten laser pulses at each location. None of the three observed zinc analyte

emission lines demonstrated any systematic trend or variation across the nail, but all did exhibit significant scatter. Shown to the right of the intensities of each emission line is the average and the standard deviation of the ten measurements. The sum of the strong Zn II lines possessed a fractional standard deviation (defined as the one-sigma standard deviation divided by the average) of 0.26. The SEM-EDS measurements described in Section 2.5 confirmed this lateral uniformity. Fig. 3b shows a 1.4 mm line scan of the Kα zinc signal comprising 1400 measurements which spanned five LIBS craters (visible above the superimposed Kα signal in the image). Below the SEM image is the Kα data, showing no systematic change in zinc concentration laterally.

To determine if it was appropriate to average ten sequential laser shots fired in one location on the nail, the depth dependence of the LIBS zinc emission was studied. Spectra were acquired from single LIBS laser pulses and 15 pulses were fired in one location. Fig. 4a shows the region around the Zn II emission line at 202 nm for the 15 spectra with four specific spectra denoted. Fig. 4b plots the measures LIBS zinc intensity of the three analyte lines and gives the average and standard deviation of the 15 measurements. In this specimen, no systematic behavior with depth was observed and the emission from shot #15 (taken last) was essentially as strong as the emission from shot #1 (taken first), while the emission from shot #14 was the weakest. This should be interpreted as typical shot-to-shot variation, not a true variation of LIBS intensity with depth. The actual depth of the laser shots is unknown, the SEM being unable to yield accurate depth information. Multiple nail specimens were studied in this way and no consistent correlation with depth was overserved in any of the samples tested, however no more than 15 laser shots were ever used in any one location. The data shown in Figure 4 were chosen as representative.

3.3. Comparison of Fingers and Hands

The LIBS zinc intensity as defined in 3.1 was obtained from clippings from the index, middle, and ring fingers of both hands of five subjects: S1, S2, S3, S4, and S6. Samples from subject 5 were excluded due to lack of a complete set of nails from all fingers. Fig. 5a shows the average measured LIBS zinc intensity from ten measurements on each finger. The error bars are the one-sigma standard deviations of those averages. There was no observed systematic trend in the nails obtained from any specific finger and due to the large shot-to-shot variation in the LIBS spectra there was no statistical difference between nails obtained from the three fingers of each subject. Therefore the three fingers were averaged together to obtain a single averaged value for each subject's left-hand (L) and right-hand (R), shown in Fig. 5b. Each value is an average of 30 spectra or 1500 total laser shots and the error bars are the one-sigma standard deviation of those 30 spectra.

The values for left and right hand were also consistent within their uncertainty (5b), therefore it was deemed to be appropriate to combine the left and right hand data into a single measurement of zinc intensity for the subject. This is shown in Fig. 5c which is the average of 60 spectra or 3000 total laser shots. Despite the large number of laser shots, the scatter of the measurements is still large, with an average fractional uncertainty of approximately 0.28. To reduce this measurement shot noise, the zinc intensity of each spectrum was normalized to the carbon emission intensity as described in section 3.1. The result of this is shown in Fig 5d, which shows that the normalization is effective at slightly improving the precision of the zinc quantification, reducing the fractional uncertainty to approximately 0.21, while not distorting the qualitative performance of the assay.

3.4. Effect of Hydration

A fractional uncertainty exceeding 0.20 (20% noise on the measurement) is not intrinsic to the LIBS method. The fractional uncertainty of a flat stainless steel calibration standard measured daily using this same apparatus over many months was approximately 0.05, or 5%, although it can be larger for less intense emission lines. It is known that the presence of water in a sample can have an impact on the formation of the LIBS plasma and therefore its temperature and emission intensity. A study was conducted to see if the influence of the state of hydration of the nail sample was responsible for the observed shot-to-shot-variation. Nails were soaked in water to over-hydrate them prior to testing as described in section 2.4. Three soaked samples (denoted "wet" A-C in Fig. 6 and plotted with a filled column) and three control samples (denoted "control" A-C in Fig. 6 and plotted with an open column) were tested using the standard protocol of section 2.3. Fig. 6a shows no systematic effect of the soaking on the LIBS zinc emission. The presence of liquid water in the nail sample should serve to reduce the overall LIBS emission intensity and specifically reduce the emission intensity from the zinc ions due to a substantially lower plasma temperature. In fact, soaking increased the emission intensity in two of the cases (subjects A and B) and decreased the emission intensity in one case (subject C) although none of these changes was significant within the uncertainty of the measurement. If the water was stored in small heterogeneous microscopic pockets within the nail structure, it was hoped that alternation of the amount of water content would impact the shot-to-shot variability of the LIBS measurements as well as the overall intensity. Fig. 6b shows no systematic increase or decrease in the fractional standard deviation of the nail measurements. In one case (subject B) the soaked sample exhibited significantly greater scatter of the measurements; in one case (sample C) the soaked sample exhibited significantly reduced scatter; and in one case (subject A) almost no difference was

observed. These results are consistent with no reproducible systematic effect due to the attempt to overhydrate the nail samples via extended soaking.

To investigate the effect of extreme drying, nail samples obtained from the same three subjects, A, B, and C were dehydrated as described in section 2.4 (denoted "dried" A-C in Fig. 7 and plotted with a filled column). Standard nail samples were also tested as a control (denoted "control" A-C in Fig. 7 and plotted with an open column). This attempt to dehydrate the nail samples also did not systematically alter the LIBS zinc emission as shown in Fig. 7a, with one case (sample B) showing significantly decreased intensity; one case (sample C) showing slightly greater intensity; and one case (sample A) showing approximately no change. Again, any observed shift was not statistically significant within the uncertainty of the measurements. Similarly, dehydration did not reduce the shot-to-shot variation of the measurements as anticipated as shown in Fig. 7b. One sample (B) showed a significant decrease in the scatter of the measurements, but the other two showed slight increases.

The results of these experiments imply that the state of hydration of the nails was not the most significant factor in determining the overall zinc emission intensity in the plasma or the observed variation in measured intensity. This is fortuitous, as nails tested in any future in situ LIBS nail analysis device used for clinical screening will not be controlled as rigorously as the "controls" in these experiments. However, these nails will also not be exposed to the extreme conditions of hydration or dehydration utilized in these experiments which appeared to have little reproducible effect.

3.5. Effect of Surface Roughness

To determine if the intrinsic surface roughness of the nail contributed significantly to the observed shot-to-shot scatter, nails were mechanically buffed smooth as described in section 2.2. Fig. 8 shows SEM images of the control (8a) and smoothed (8b) nail, as well as the average Zn II LIBS emission intensity from each of these two samples (8c). Four ablation craters on a square grid are visible in both 8a and 8b and the difference in surface roughness due to the buffing is appreciable, although it was not quantified. Both samples yielded identical LIBS Zn II emission intensity within uncertainty (8c), but the buffed nail possessed significantly reduced scatter in the measurements. The control nail had an average Zn II emission intensity of 1097.9 ± 221.2 a.u. while the buffed nail had an average Zn II emission intensity of 1076 ± 122.3 a.u. Buffing reduced the fractional standard deviation by almost 50% from 0.20 to 0.11. As this test was not performed until near the end of the investigation, buffing was not added to the standard preparation protocol of the nails, but will be in future studies. To determine if buffing left any residue on the nails that could be detected by LIBS, a qualitative analysis of the nail buffer was performed. Consistent Ti emission was observed in the nail buffer spectra but not in the nail spectra, indicating that if the nail buffer left any residue on the nails, it was removed during the ultrasound cleaning process described above.

The larger than expected deviation of the LIBS measurements made on a single nail specimen can be explained by non-uniform ablation by the 1064 nm Nd:YAG laser due to the structure of the fingernail. Fig. 9a shows a 60x magnification SEM image of an array of single-shot LIBS craters formed in a nitrocellulose filter medium by our apparatus and Fig. 9b is a magnified view of one ablation crater in this filter medium showing a diameter of approximately 65 microns. For

comparison, Fig. 9c shows a single shot LIBS crater in our stainless steel calibration plate under 250x magnification, while 9d shows the same type of ablation on the fingernail, at the same 250x magnification. The differences in size and uniformity due solely to the laser-material interaction are immediately apparent. Fig. 9e shows a 70x magnification SEM image of a 5x5 grid of LIBS craters in a fingernail and Fig. 9f is a magnified view of the ablation structure outlined by the square in 9e. Each crater was created by ten laser pulses in each location. It is readily apparent that the uniformity of the ablation process in the filter medium and steel is high, while in the fingernail no two ablation events appear identical or even similar. In the center of the nail on the left of Fig. 9e the laser appears to have ablated almost no material at all, resulting in no obvious crater, while on the right side of the image in 9e the laser appears to have caused the layered nail structure to peel back (shown in a magnified view in Fig. 9f) or flake away in a highly uncontrolled and irreproducible way. The damage to the nail material also exhibited a directional inhomogeneity, as evidenced by the tendency of ablation features to stretch diagonally from the upper left corner of 9e to the lower right corner. No such directional asymmetry is present in the apparatus, as evidence by the highly circular ablation shown in 9a, 9b, and 9c. Similar ablation was observed in all the nail samples tested in this study. Thus the layered nature and the fibrous structure of the fingernails were responsible for the non-uniform ablation observed in figure 9, which explains the scatter observed in the measurements reported in this manuscript.

This behavior may also explain the observation by Rusack et al.[31] that pressed keratin pellets were not an effective LIBS calibration standard for a LIBS fingernail assay using a 1064 nm laser. Pressed keratin pellets created from a uniform homogenous powder would possess no such

asymmetrical striations or vertical layering, yielding more reproducible ablation, but not effectively modeling the behavior of a true fingernail.

It is believed that the weak interaction of the 1064 nm Nd:YAG with the keratin nail is responsible for this effect, allowing the ablation to occur or initiate at depth rather than in a more controlled manner on or near the surface of the nail. Experiments are underway to replace the 1064 nm laser with the quadrupled and tripled Nd:YAG harmonics at 266 nm and 355 nm, respectively. The absorption coefficient of bulk keratin is greater at both of these wavelengths than at 1064 and the absorption at 266 nm is approximately 10 times greater than at 355.[35] As shown, however, the ablation properties of bulk keratin and human fingernails may not correlate well, and we know of no published reports of ultraviolet LIBS performed on fingernails.

3.6 Calibration via Multivariate analysis

Absolute zinc concentrations for the five tested nail samples were obtained by speciated isotope dilution mass spectrometry (SIDMS). A partial least squares (PLS) regression (PLS_Toolbox, Eigenvector, Inc.) was performed on the data using the 30 left hand measurements from each subject to create the regression model and using the 30 right hand measurements to test the model. It was assumed that all the fingers possessed the same zinc concentration, although only nails from one finger were tested with SIDMS for each subject. The results of the analysis are shown in Table 1 and Figure 10. Figure 10 is a plot of the average predicted PLS concentration versus the actual SIDMS concentrations. The error bars are the one-sigma standard deviations of the 30 predictions (given in Table 1) and the line is a linear fit to the predictions possessing a Pearson's R of 0.945 and an adjusted R-squared of 0.858. Taken in toto, the five predictions differed from the actual

concentrations by an average of 6.8 ppm (an average percent uncertainty of 5%), well below the one-sigma uncertainty. The average standard deviation exhibited by all the predictions was 14 ppm, with an average fractional uncertainty on the predictions of 12%.

4. Conclusions

Nutritional zinc present in human fingernails is quantifiable using the very rapid assay of laser-induced breakdown spectroscopy (LIBS). LIBS measurements performed on human nail clippings with a 1064 nm laser exhibited a high degree of variability and intrinsic measurement scatter that was found to not depend upon the state of hydration of the nail, the lateral position sampled across the nail, or the depth within the nail at which the plasma is formed (up to a depth achieved by 15 laser pulses). Surface roughness was found to be a contributing factor, and buffing the nail smooth prior to testing reduced the standard deviation of the measurements by a factor of almost two. Normalization of the LIBS zinc intensity by other LIBS spectra emission features, specifically the intense carbon emission at 247 nm, was not found to significantly improve measurement accuracy or precision in this protocol. Non-uniform ablation due to the layered nature and the fibrous structure of the fingernails was observed by scanning electron microscopy in all the samples tested in this study and was found to be the dominant source of measurement uncertainty. In spite of this, a partial least squares regression model built from the left hand zinc measurements of five subjects was constructed and used to test the right hand zinc measurements, yielding predictions that differed from the actual concentration by an average of 6.8 ppm and possessing a standard deviation of 14 ppm, or 12% fractional uncertainty.

A study with a greater number of overall participants which includes a pool of "zinc deficient" participants now needs to be conducted. Still, these preliminary results are highly encouraging for future in situ screening measurements, as the fingernail content of subjects with low zinc nutriture are expected to be as much as 50 ppm lower than that of subjects with exemplary zinc intake. Therefore, while the uncertainty of the measurements as shown in figure 10 is relatively large and may preclude precise zinc quantification in finger nails, the uncertainty obtained in these experiments would still allow a rapid determination of deficient or non-deficient on the basis of the LIBS measurement alone which was the intent of this study.

The LIBS measurement is not only more convenient and simpler to perform than the traditional blood serum measurement, but it is also expected to be much more robust and indicative of zinc nutritional status. The serum measurement is unreliable and simply not indicative of zinc nutritional status because serum zinc varies strongly with the time of day and in response to diet (the time of eating as well as the glucose content) and also other physiologic conditions such as intestinal disease, pregnancy, infection and even strenuous physical exercise.[36]

It is believed that performing the LIBS measurements with ultraviolet wavelength lasers that are attenuated much more readily by the nail material yielding more intense plasmas and more controlled laser ablation will provide an even greater amount of measurement stability which is necessary to reduce the observed shot-to-shot variation even further. In addition, the increased LIBS intensity and reproducibility would allow a decrease in the number of laser shots or accumulated spectra required to accurately quantify fingernail zinc in a rapid screening diagnostic.

Acknowledgements

The authors would like to thank William I. Manton, Ph.D. (UT Dallas & NeuroBioTex, Inc.) for performing the SIDMS measurements. The authors gratefully acknowledge the financial support of a Natural Sciences and Engineering Research Council of Canada Discovery grant and RTI equipment grant as well as a Canada Foundation for Innovation – Ontario Innovation Fund infrastructure grant. VR was supported by both the University of Windsor's Outstanding Scholars program and an NSERC USRA scholarship.

[1] B.K.Y Bitanihirwe, M.G. Cunningham. “Zinc: The brain’s dark horse”. Synapse. 2009. 63(11): 1029-1049.

[2] C.J. Frederickson, J.Y. Koh, A.I. Bush. “The neurobiology of zinc in health and disease”. Nat. Rev. Neurosci. 2005. 6(6): 449–462.

[3] N. Roohani, R. Hurrell, R. Kelishadi, R. Schulin. “Zinc and its importance for human health: An integrative review”. J. Res. Med. Sci. 2013. 18(2): 144-157.

[4] R.L. Bailey, K.P. West, Jr., R.E. Black. “The epidemiology of global micronutrient deficiencies.” Ann. Nutr. Metab. 2015. 66(Suppl 2): 22-33.

[5] N.F. Krebs, L.V. Miller, K.M. Hambidge. “Zinc deficiency in infants and children: a review of its complex and synergistic interactions”. Paediatr. Int. Child Health. 2014. 34(4): 279-288.

[6] S. Horton, F. Begin, A. Greig, A. Lakshman. Best practice paper: Micronutrient supplements for child survival (vitamin A and zinc). Copenhagen Consensus Center, 2008.

[7] C.J. Frederickson, S.W. Suh, D. Silva, C.J. Frederickson, R.B. Thompson. “Importance of zinc in the central nervous system: The zinc containing neuron”. J. Nutr. 2000. 130(5): 1471S–1483S.

[8] S.L. Sensi, P. Paoletti, A.I. Bush, I. Sekler. “Zinc in the physiology and pathology of the CNS”. Nat. Rev. Neurosci. 2009. 10(11): 780-791.

[9] S.L. Sensi, P. Paoletti, J.Y. Koh, E. Aizenman, A.I. Bush, M. Hershfinkel. “The neurophysiology and pathology of brain zinc”. J. Neurosci. 2011. 31(45): 16076-16085.

[10] F.M. Burnet. “A possible role of zinc in the pathology of dementia”. Lancet 1981. 1(8213): 186-188.

[11] I. Shcherbatykh, D.O. Carpenter. “The role of metals in the etiology of Alzheimer’s disease”. J. Alzheimers Dis. 2007. 11(2): 191-205.

[12] E.J. Lee, H. Lee, T.N. Huang, C. Chung, W. Shin, K. Kim, J.Y. Koh, Y.P. Hsueh, E. Kim. "Trans-synaptic zinc mobilization improves interaction in two mouse models of autism NMDAR activation". Nat. Comm. 2015. 6(7168): 1-12.

[13] S. Meret, R.I. Henkin. "Simultaneous direct estimation by atomic absorption spectrophotometry of copper and zinc in serum, urine, and cerebrospinal fluid". Clin. Chem. 1971 17(5): 369-373.

[14] H.H. Sandstead, A.S. Prasad, J.G. Penland, F.W. Beck, J. Kaplan, N.G. Egger, N.W. Alcock, R.M. Carroll, V.M. Ramanujam, H.H. Dayal, C.D. Rocco, R.A. Plotkin, A.N. Zavaleta. "Zinc deficiency in Mexican American children: influence of zinc and other micronutrients on T cells, cytokines, and anti-inflammatory plasma proteins". Am. J. Clin. Nutr. 2008. 88(4): 1067-1073.

[15] The Mayo Clinic. "Drugs and Supplements: Zinc." Information accessed on August 18, 2015 and recommendations last updated on Nov. 01, 2013. http://www.mayoclinic.org/drugs-supplements/zinc/dosing/HRB-20060638

[16] J. Salgueiro, N. Leonardi, M. Zubillaga, R. Weill, C. Goldman, G. Calmanovici, A. Barrado, M.M. Sarrasague, J. Boccio. "Determination of relative bioavailability of zinc in a petit suisse cheese using weight gain and bone zinc content in rats as markers". Biol. Trace Elem. Res. 2005. 104(3): 261-267.

[17] J.H. Park, C.J. Grandjean, D.L. Antonson, J.A. Vanderhoof. "Effects of isolated zinc deficiency on the composition of skeletal muscle, liver and bone during growth in rats". J. Nutr. 1986. 116(4): 610-617.

[18] L. Morini, E. Marchei, L Tarani, M. Trivelli, G. Rapisardi, M.R. Elicio, J. Ramis, O. Garcia-Algar, L. Memo, R. Pacifici, A. Groppi, P. Danesino, S. Pichini. "Testing ethylglucuronide in

maternal hair and nails for the assessment of fetal exposure to alcohol: comparison with meconium testing". Ther. Drug Monit. 2013. 35(3): 402-407.

[19] M. Longnecker, M.J. Stampfer, J.S. Morris, V. Spate, C. Baskett, M. Mason, W.C. Willett. "A 1-y trial of the effect of high-selenium bread on selenium concentrations in blood and toenails". Am. J. Clin. Nutr. 1993. 57(3): 408-413.

[20] W.K. Al-Delaimy, G.N. Mahoney, F.E. Speizer, W.C. Willett. "Toenail nicotine levels as a biomarker of tobacco smoke exposure". Cancer Epidem. Biomar. 2002. 11(11): 1400-1404.

[21] M. Garland, J.S. Morris, B.A. Rosner, M.J. Stampfer, V.L. Spate, C.J. Baskett, W.C. Willett, D.J. Hunter. "Toenail trace element levels as biomarkers: reproducibility over a 6-year period". Cancer Epidem. Biomar. 1993. 2(5): 493-497.

[22] K.M. Hambidge, C. Hambidge, M. Jacobs, J.D. Baum. "Low levels of zinc in hair, anorexia, poor growth, and hypogeusia in children". Pediatr. Res. 1972. 6(12): 868-874.

[23] X. Wu, J. Tang, M. Xie. "Serum and hair zinc levels in breast cancer: a meta-analysis". Sci. Rep. 2015. 5(12249): 1-8.

[24] C.J. Frederickson, W.I. Manton, M. Baudelet, M. Richardson, C. Jeon, S.J. Rehse , V.A. Riberdy, A.S. Prasad, R.A. McLauchlan, C.J.M. Frederickson, M. Zaman, N. Lowe. "A field-portable device for rapid determination of nutritional and toxic metal status by fingernail analysis". Heal. Technol. Paper submitted, 2016.

[25] B.L. Batista, J.L. Rodrigues, J.A. Nunes, L. Tormen, A.J. Curtius, F. Barbosa, Jr. "Simultaneous determination of Cd, Cu, Mn, Ni, Pb and Zn in nail samples by inductively coupled plasma mass spectrometry (ICP-MS) after tetramethyl ammonium hydroxide solubilization at room temperature: Comparison with ETAAS". Talanta. 2008. 76(3): 575-579.

[26] D.E.B. Fleming, M.R. Gherase, M. Anthonisen. “Calibrations for measurement of manganese and zinc in nail clippings using portable XRF.” X-Ray Spectrom. 2013. 42(4): 299–302.

[27] Z. Hosseinimakarem, S.H. Tavassoli. “Analysis of human nails by laser-induced breakdown spectroscopy”. J. Biomed. Opt. 2011. 16(5): 057002-057002.

[28] M. Bahreini, S.H. Tavassoli. “Possibility of thyroidism diagnosis by laser induced breakdown spectroscopy of human fingernail”. J. Lasers Med. Sci. 2012. 3(3): 127-131.

[29] S. Hamzaoui, R. Khleifia, N. Jaïdane, Z. Ben Lakhdar. “Quantitative analysis of pathological nails using laser-induced breakdown spectroscopy (LIBS) technique”. Lasers Med. Sci. 2011. 26(1): 79-83.

[30] S. Shadman, M. Bahreini, S.H. Tavassoli. “Comparison between elemental composition of human fingernails of healthy and opium addicted subjects by laser-induced breakdown spectroscopy”. Appl. Opt. 2012. 51(12): 2004-2011.

[31] D.A. Rusak, A.E. Zeleniak, J.L. Obuhosky, S.M. Holdren, C.A. Noldy. “Quantitative determination of calcium, magnesium, and zinc in fingernails by laser-induced breakdown spectroscopy”. Talanta. 2013. 117: 55-59.

[32] S.J. Rehse, J. Diedrich, S. Palchaudhuri. Identification and discrimination of *Pseudomonas aeruginosa* bacteria grown in blood and bile by laser-induced breakdown spectroscopy. Spectrochim. Acta B. 2007. 62(10): 1169-1176.

[33] D.J. Malenfant, D. Gillies, S.J. Rehse. “Bacterial suspensions deposited on microbiological filter material for rapid laser-induced breakdown spectroscopy identification”. Appl. Spect. 2016. 70(3): 485-493.

[34] S.O. Olabanji, O.A. Ajose, N.O. Makinde, M.C. Buoso, D. Ceccato, M. De Poli, G. Moschini. "Characterization of human fingernail elements using PIXE technique". Nucl. Instrum. Meth. B. 2005. 240(4): 895–907.

[35] E.G. Bendit, D. Ross. "A technique for obtaining the ultraviolet absorption spectrum of solid keratin". Appl. Spectrosc. 1961. 15(4): 103-105.

[36] K.H. Brown, S.E. Wuehler, J.M. Peerson. "The importance of zinc in human nutrition and estimation of the global prevalence of zinc deficiency." Food Nutr. Bull. 2001. 22(2):113-125.

Figure captions

Fig. 1. The experimental apparatus utilized in this work.

Fig. 2. A full LIBS spectrum from a fingernail sample (a) and the spectral regions of interest (b-d).

Fig. 3. Measured LIBS zinc intensity as a function of lateral distance across the fingernail (a). Energy dispersive x-ray measurement of the zinc Kα line strength superimposed on an SEM image of the nail with LIBS craters clearly visible (b).

Fig. 4. The overlapped spectra from fifteen sequential single-shot LIBS spectra acquired in a single location (a). No consistent trend as a function of depth in the nail was observed. The measured zinc emission intensities for the 15 laser pulses (b).

Fig. 5. The averaged zinc intensity from ten measurements on each finger (middle, ring, index only) from both hands of five subjects (a). The measurements of all fingers combined per hand (b) and combined per subject (c). The measurement per subject after normalization by the carbon 247 nm line.

Fig. 6. The effect of overhydration of a fingernail specimen prior to LIBS testing on the measured LIBS zinc emission intensity (a) and the standard deviation of the intensity measurements (b).

Fig. 7. The effect of dehydration of a fingernail specimen prior to LIBS testing on the measured LIBS zinc emission intensity (a) and the standard deviation of the intensity measurements (b).

Fig. 8. Scanning electron micrographs of a control fingernail (a) and a nail smoothed by buffing (b). LIBS zinc intensity measurements were similar for both nails but the buffed nail possessed smaller scatter in the measurements (c).

Fig. 9. Scanning electron micrographs of LIBS craters formed in a nitrocellulose filter medium (a,b), a stainless steel calibration plate (c), and a fingernail (d,e,f). (b) A magnified view of the box shown in (a). (f) A magnified view of the box shown in (e).

Fig. 10. The predicted zinc concentration from five fingernail samples as a function of the actual zinc concentration as determined by SIDMS. The line is a fit to the predictions to show the linearity of the model performance (Pearson's R of 0.945).

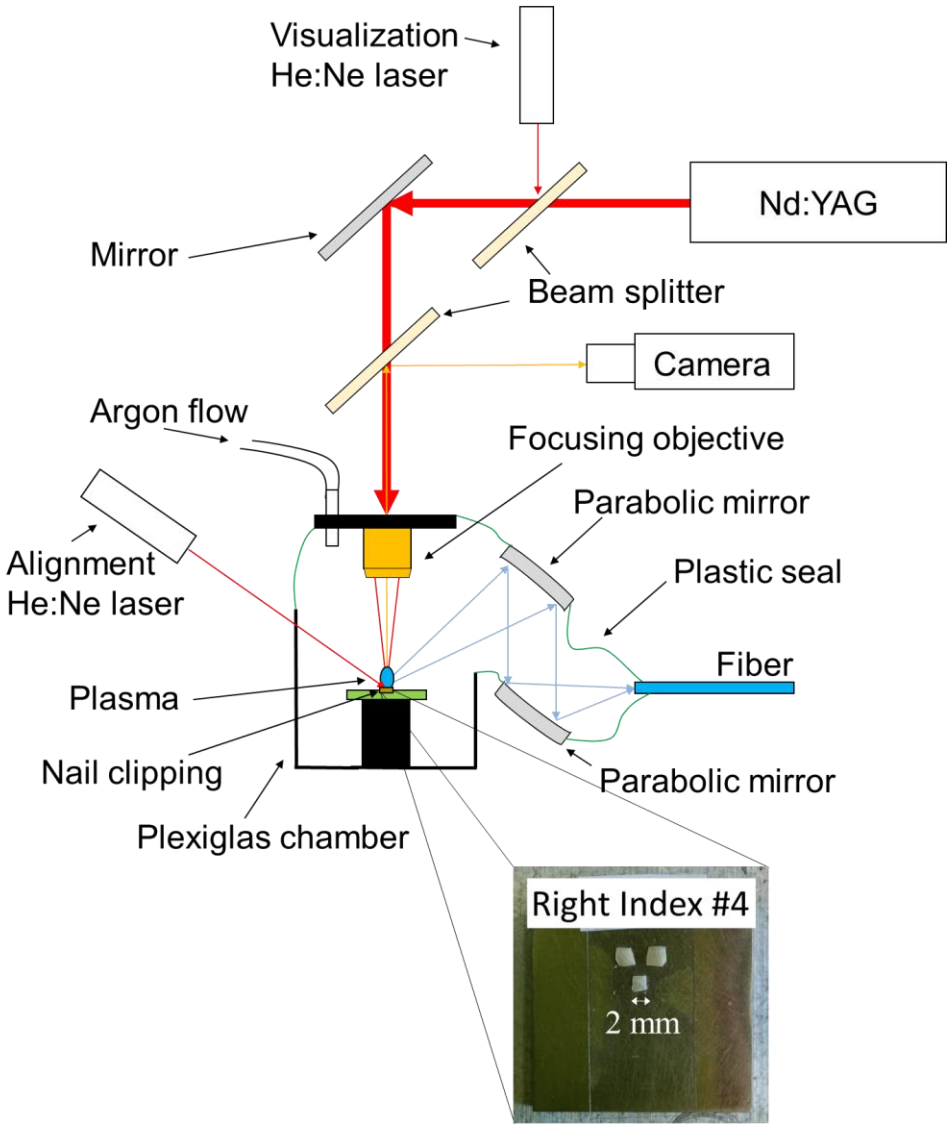
Visualization
He:Ne laser
Nd:YAG
Mirror
Beam splitter
Camera
Argon flow
Focusing objective
Parabolic mirror
Alignment
He:Ne laser
Plastic seal
Fiber
Plasma
Nail clipping
Parabolic mirror
Plexiglas chamber
Right Index #4
2 mm

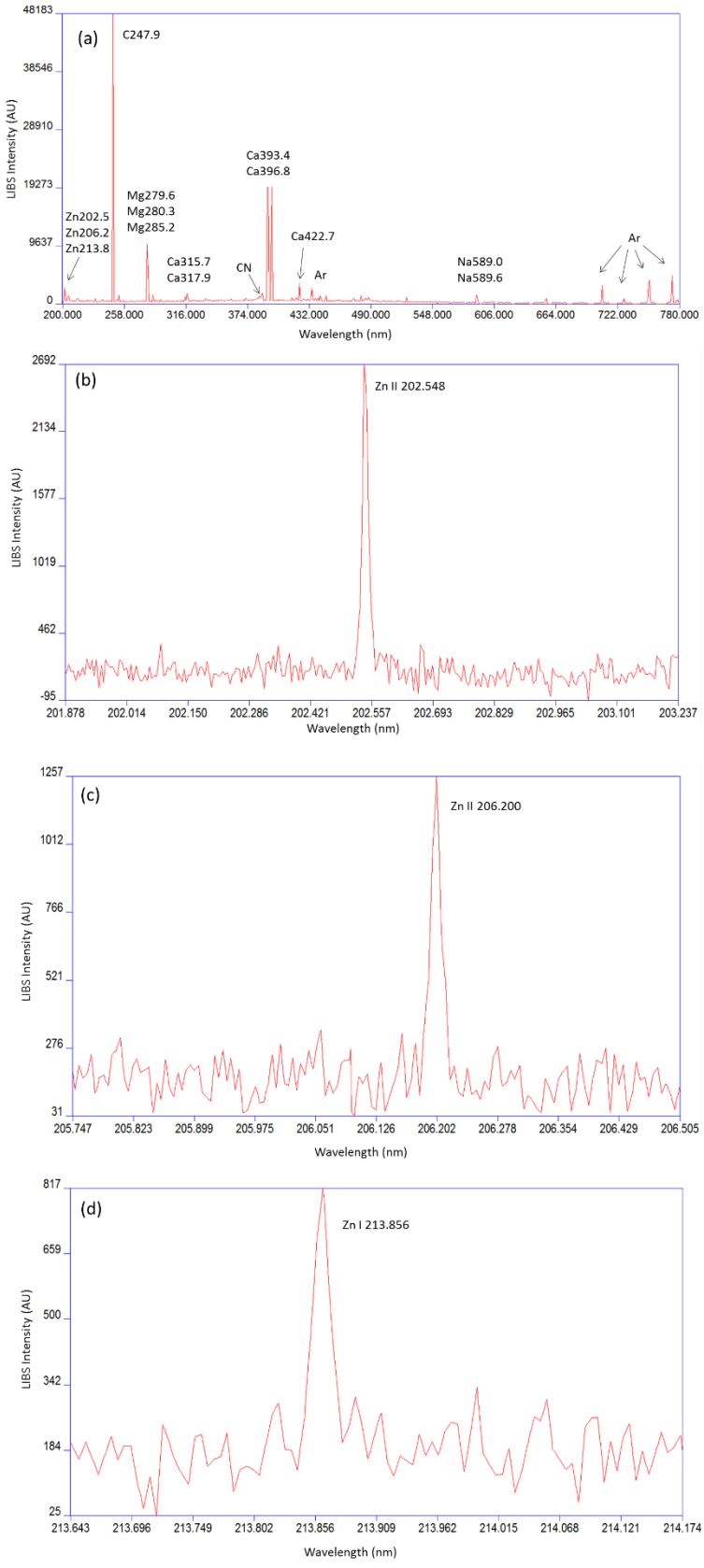
(a)
C247.9
Zn202.5
Zn206.2
Zn213.8
Mg279.6
Mg280.3
Mg285.2
Ca315.7
Ca317.9
CN
Ca393.4
Ca396.8
Ca422.7
Ar
Na589.0
Na589.6
Ar
LIBS Intensity (AU)
Wavelength (nm)
(b)
Zn II 202.548
(c)
Zn II 206.200
(d)
Zn I 213.856

(a)

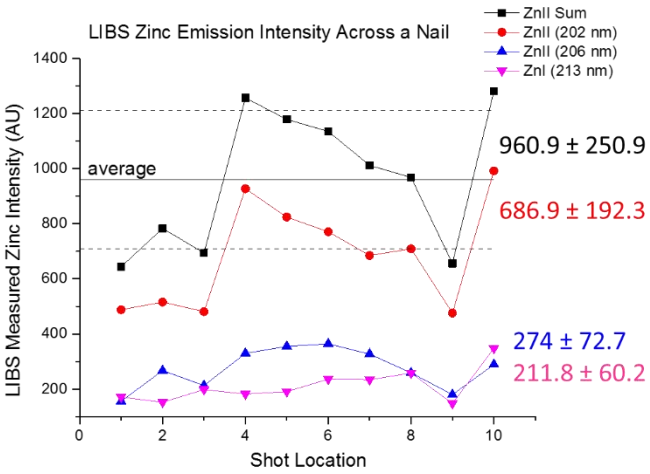
LIBS Zinc Emission Intensity Across a Nail
ZnII Sum
ZnII (202 nm)
ZnII (206 nm)
ZnI (213 nm)
LIBS Measured Zinc Intensity (AU)
1400
1200
1000
800
600
400
200
average
960.9 ± 250.9
686.9 ± 192.3
274 ± 72.7
211.8 ± 60.2
0
2
4
6
8
10
Shot Location

(b)

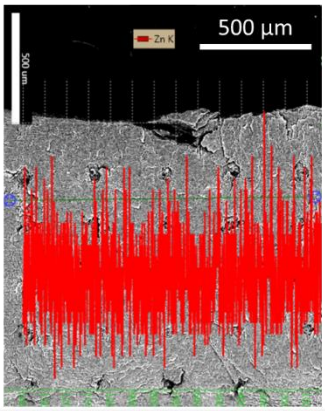
500 µm
Zn K
500 um


30
28
26
24
22
20
18
16
14
12
10
8
6
4
2
0
Roi
199
399
599
799
999
1199
Distance (µm)

(a)

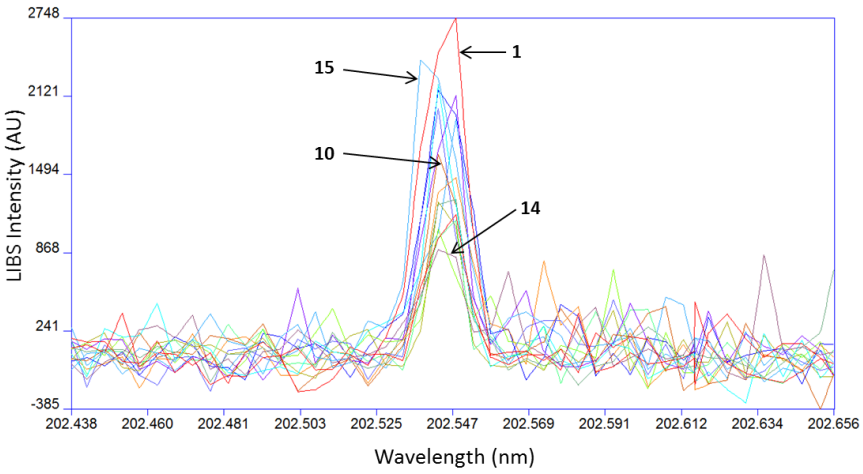
2748
2121
1494
868
241
-385
LIBS Intensity (AU)
15
1
10
14
202.438
202.460
202.481
202.503
202.525
202.547
202.569
202.591
202.612
202.634
202.656
Wavelength (nm)

(b)

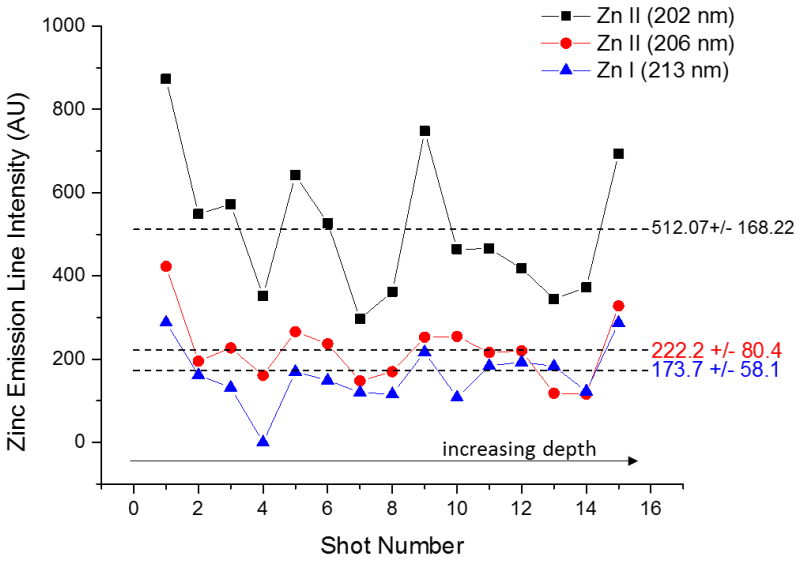
Zn II (202 nm)
Zn II (206 nm)
Zn I (213 nm)
1000
800
600
400
200
0
Zinc Emission Line Intensity (AU)
512.07+/- 168.22
222.2 +/- 80.4
173.7 +/- 58.1
increasing depth
0
2
4
6
8
10
12
14
16
Shot Number

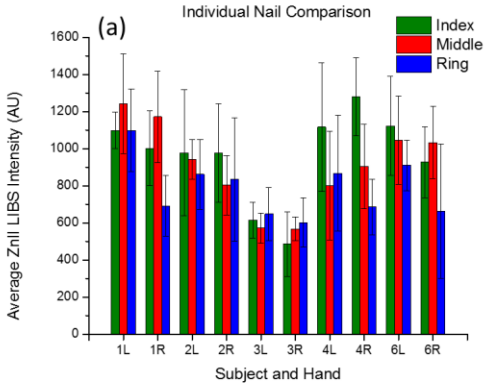
Individual Nail Comparison
(a)
Index
Middle
Ring
Average ZnII LIBS Intensity (AU)
0
200
400
600
800
1000
1200
1400
1600
1L
1R
2L
2R
3L
3R
4L
4R
6L
6R
Subject and Hand

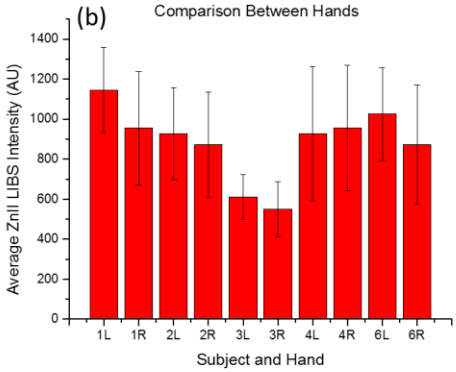
(b)
Comparison Between Hands
Average ZnII LIBS Intensity (AU)
0
200
400
600
800
1000
1200
1400
1L
1R
2L
2R
3L
3R
4L
4R
6L
6R
Subject and Hand

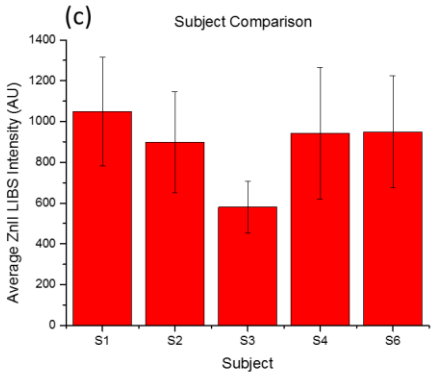
(c)
Subject Comparison
Average ZnII LIBS Intensity (AU)
0
200
400
600
800
1000
1200
1400
S1
S2
S3
S4
S6
Subject

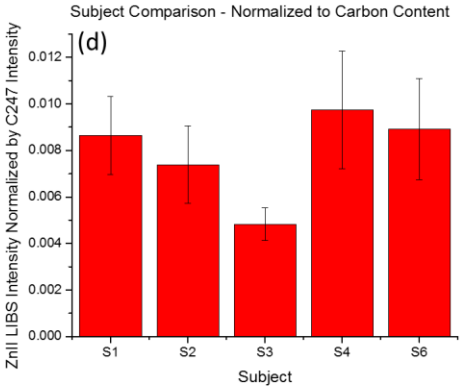
Subject Comparison - Normalized to Carbon Content
(d)
ZnII LIBS Intensity Normalized by C247 Intensity
0.000
0.002
0.004
0.006
0.008
0.010
0.012
S1
S2
S3
S4
S6
Subject

(a)

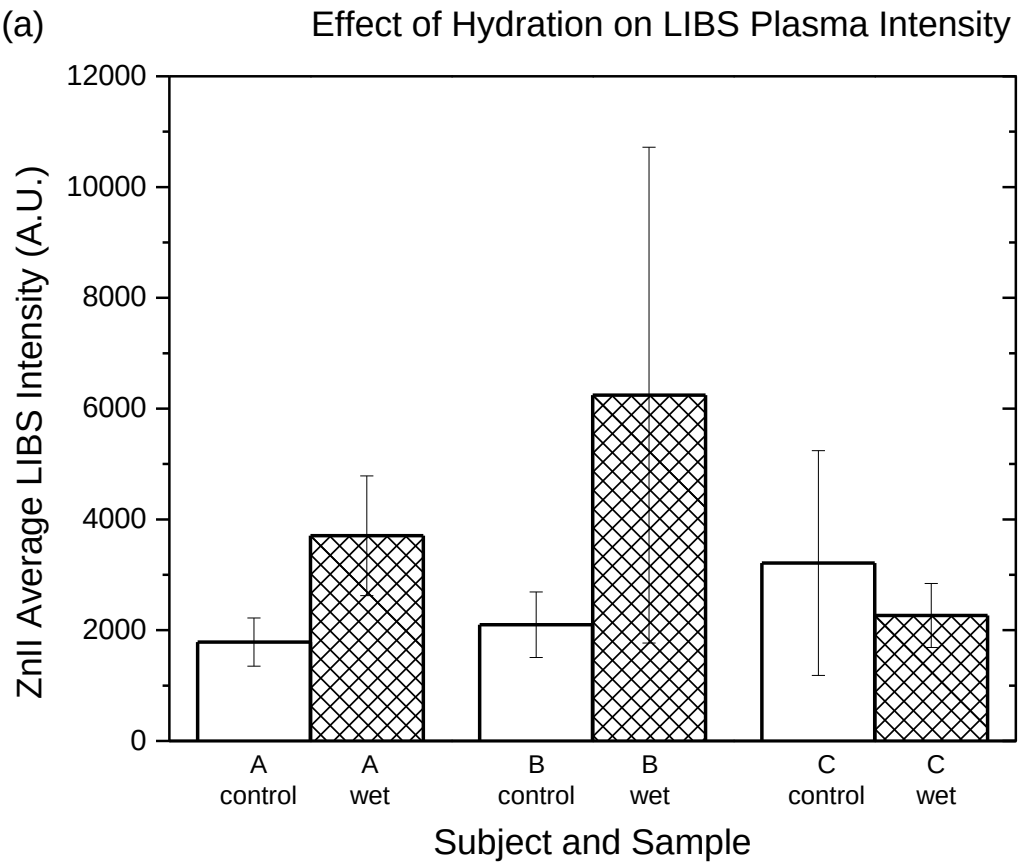
Effect of Hydration on LIBS Plasma Intensity
ZnII Average LIBS Intensity (A.U.)
12000
10000
8000
6000
4000
2000
0
A control
A wet
B control
B wet
C control
C wet
Subject and Sample

(a)

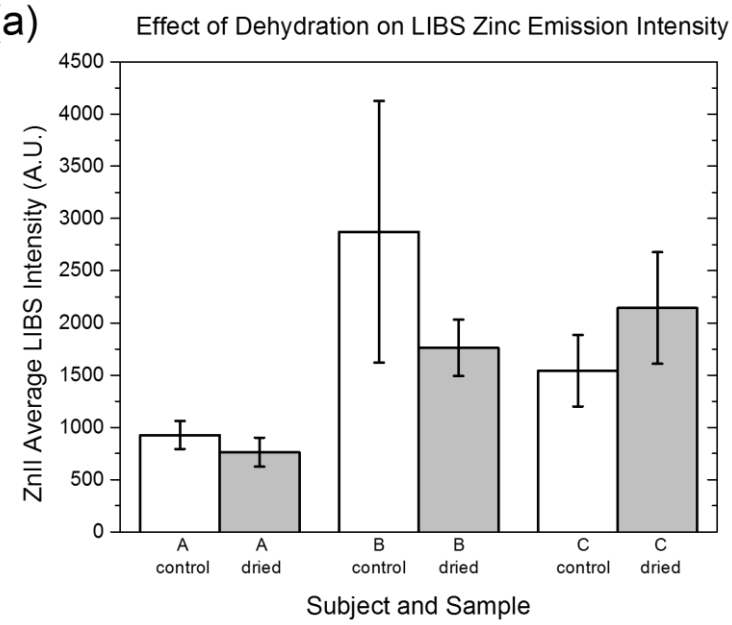
Effect of Dehydration on LIBS Zinc Emission Intensity
ZnII Average LIBS Intensity (A.U.)
4500
4000
3500
3000
2500
2000
1500
1000
500
0
A control
A dried
B control
B dried
C control
C dried
Subject and Sample

(b)

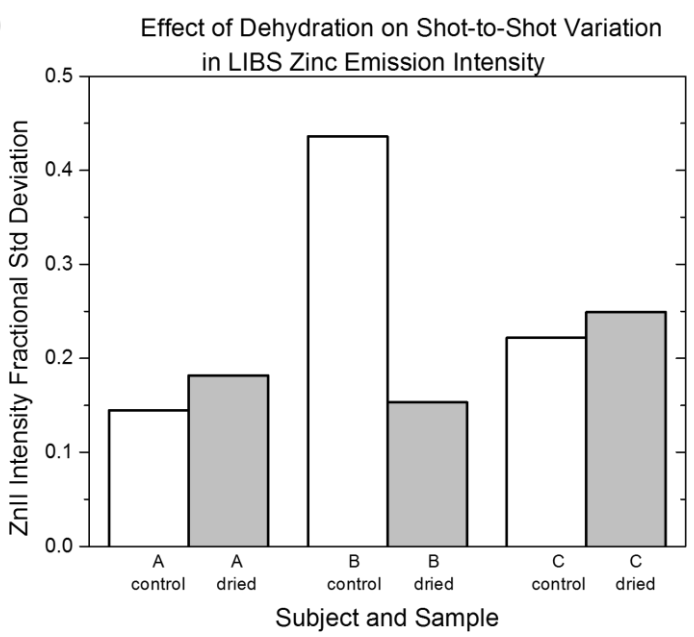
Effect of Dehydration on Shot-to-Shot Variation in LIBS Zinc Emission Intensity
ZnII Intensity Fractional Std Deviation
0.5
0.4
0.3
0.2
0.1
0.0
A control
A dried
B control
B dried
C control
C dried
Subject and Sample

(a)

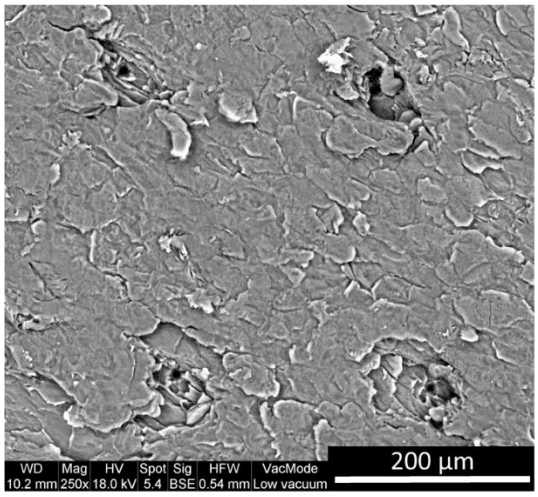
WD Mag HV Spot Sig HFW VacMode
10.2 mm 250x 18.0 kV 5.4 BSE 0.54 mm Low vacuum
200 µm

(b)

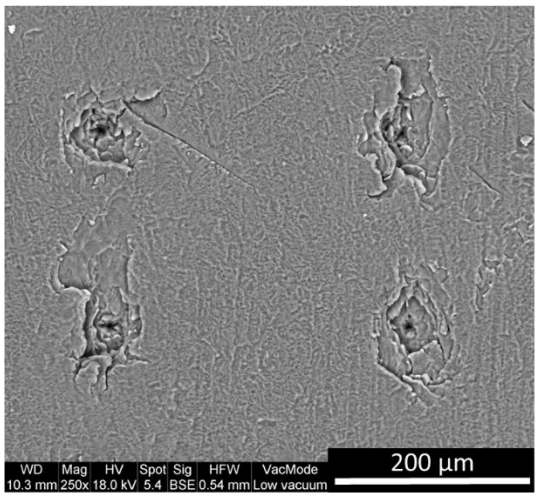
WD Mag HV Spot Sig HFW VacMode
10.3 mm 250x 18.0 kV 5.4 BSE 0.54 mm Low vacuum
200 µm

(c)

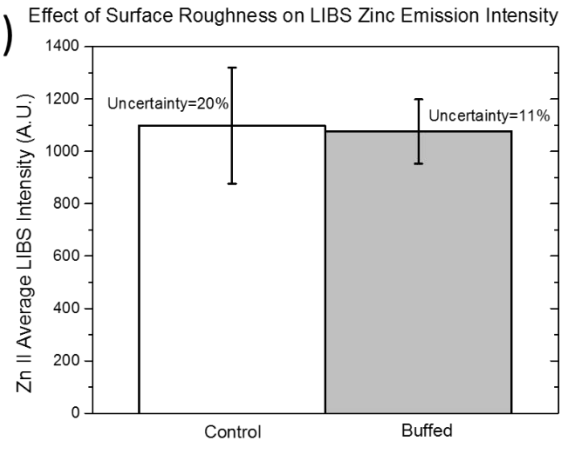
Effect of Surface Roughness on LIBS Zinc Emission Intensity
Zn II Average LIBS Intensity (A.U.)
1400
1200
1000
800
600
400
200
0
Uncertainty=20%
Uncertainty=11%
Control
Buffed

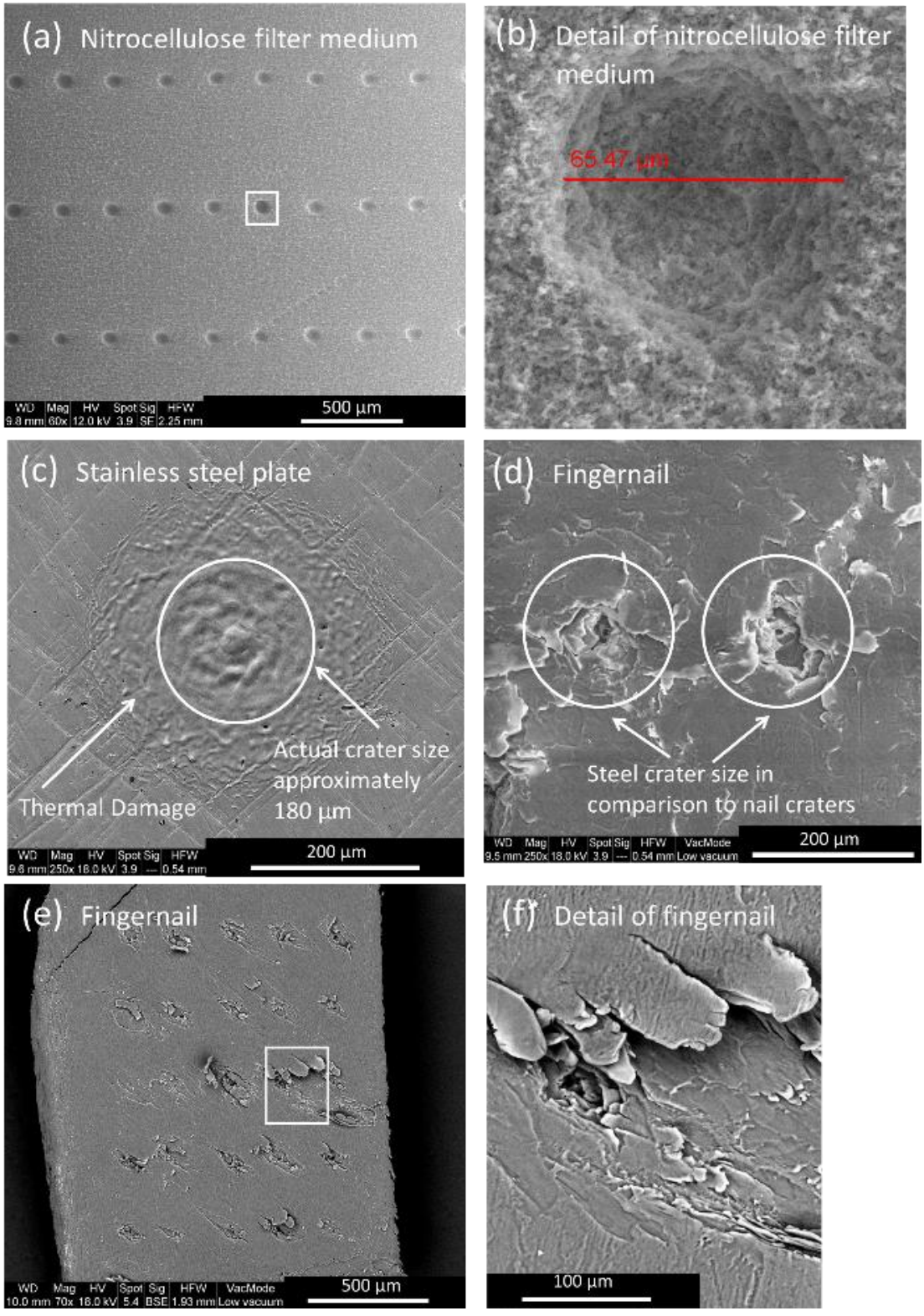
(a) Nitrocellulose filter medium
WD Mag HV Spot Sig HFW
9.8 mm 60x 12.0 kV 3.9 SE 2.25 mm
500 µm
(b) Detail of nitrocellulose filter medium
65.47 µm
(c) Stainless steel plate
Thermal Damage
Actual crater size approximately 180 µm
WD Mag HV Spot Sig HFW
9.6 mm 250x 18.0 kV 3.9 --- 0.54 mm
200 µm
(d) Fingernail
Steel crater size in comparison to nail craters
WD Mag HV Spot Sig HFW VacMode
9.5 mm 250x 18.0 kV 3.9 --- 0.54 mm Low vacuum
200 µm
(e) Fingernail
WD Mag HV Spot Sig HFW VacMode
10.0 mm 70x 18.0 kV 5.4 BSE 1.93 mm Low vacuum
500 µm
(f) Detail of fingernail
100 µm

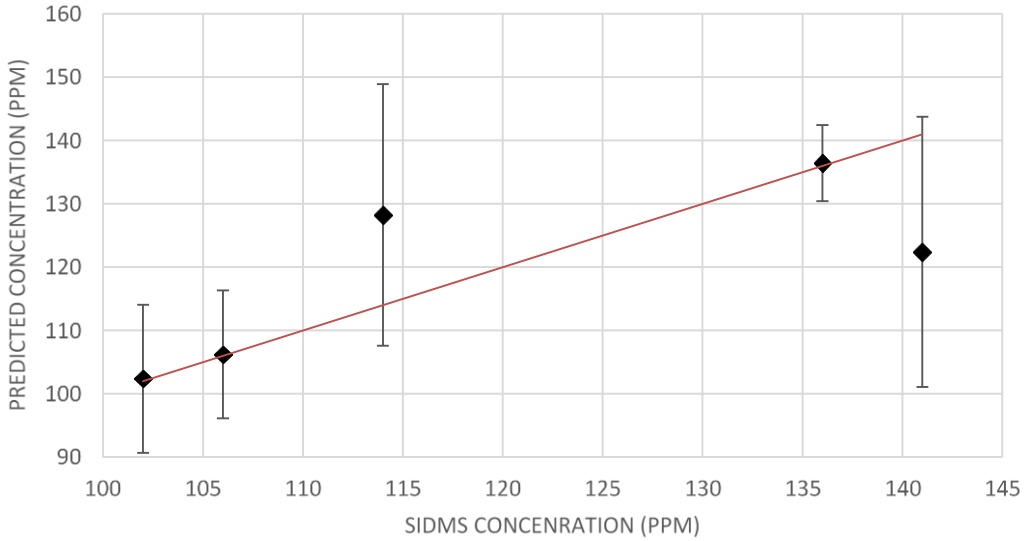
160
150
140
130
120
110
100
90
PREDICTED CONCENTRATION (PPM)
100
105
110
115
120
125
130
135
140
145
SIDMS CONCENRATION (PPM)